Acta Tropica 239 (2023) 106837

Contents lists available at ScienceDirect

Acta Tropica

journal homepage: www.elsevier.com/locate/actatropica

Linking mathematical models and trap data to infer the proliferation, abundance, and control of *Aedes aegypti*

Jing Chen [1,a], Xi Huo [1,b], André B.B. Wilke [c], John C. Beier [d], Chalmers Vasquez [e], William Petrie [e], Robert Stephen Cantrell [b], Chris Cosner [b], Shigui Ruan [b,*]

[a] Department of Mathematics, Nova Southeastern University, 3301 College Ave, Fort Lauderdale, FL 33314, USA
[b] Department of Mathematics, University of Miami, 1365 Memorial Drive, Coral Gables, FL 33146, USA
[c] Laboratory for Computational Epidemiology and Public Health, Department of Epidemiology and Biostatistics, Indiana University School of Public Health, Bloomington, IN 47405, USA
[d] Department of Public Health Sciences, Miller School of Medicine, University of Miami, Miami, FL 33136, USA
[e] Miami-Dade County Mosquito Control Division, Miami, FL 33178, USA

ARTICLE INFO

Keywords:
Aedes aegypti
mosquito control
vector-borne disease
mathematical modeling
population dynamics

ABSTRACT

Aedes aegypti is one of the most dominant mosquito species in the urban areas of Miami-Dade County, Florida, and is responsible for the local arbovirus transmissions. Since August 2016, mosquito traps have been placed throughout the county to improve surveillance and guide mosquito control and arbovirus outbreak response. In this paper, we develop a deterministic mosquito population model, estimate model parameters by using local entomological and temperature data, and use the model to calibrate the mosquito trap data from 2017 to 2019. We further use the model to compare the *Ae. aegypti* population and evaluate the impact of rainfall intensity in different urban built environments. Our results show that rainfall affects the breeding sites and the abundance of *Ae. aegypti* more significantly in tourist areas than in residential places. In addition, we apply the model to quantitatively assess the effectiveness of vector control strategies in Miami-Dade County.

1. Introduction

Aedes aegypti is the primary vector responsible for the transmission of several arboviruses, including dengue fever, chikungunya, yellow fever, and Zika fever. It is commonly found in tropical and subtropical areas and is one of the most widespread mosquito species. Urbanization and human movement are highly related to the presence and distribution of *Ae. aegypti* mosquitoes which almost exclusively feed on humans (Ponlawat and Harrington, 2005; Wilke et al., 2021a) - making them extremely threatening in terms of spreading emerging and re-emerging vector-borne diseases. Dengue, chikungunya, and Zika have been introduced into Florida, caused local outbreaks (dengue in 2010 and 2020, chikungunya in 2014, Zika in 2016), and posed a major public health problem there since *Ae. aegypti* mosquitoes are widely distributed throughout Florida. *Ae. aegypti* mosquitoes prefer artificial aquatic habitats such as flower vases, tires, barrels, cans, and bottles, posing a significant challenge against most mosquito control programs. Mosquito relative abundance is usually monitored via either mechanical traps that attract female adults seeking hosts or ovitraps that attract female adults to lay their eggs. Whenever vector control interventions are carried out, mosquito trap data collected before and after the interventions can serve as the primary resource for evaluation and assessment.

Since August 2016 during the Zika outbreak, the Miami-Dade County Mosquito Control surveillance network have placed BG-Sentinel traps (BioGents Corporation, Regensburg, Germany) to monitor the local adult mosquito population. BG-Sentinel traps that are enhanced with CO_2 released from dry ice in a small cooler are the gold standard for collecting several mosquito species including *Ae. aegypti* (Wilke et al., 2019a). The surveillance network covered the totality of Miami-Dade County, with particular attention given to the areas affected by the 2016 Zika outbreak and high human mobility: Miami Beach, Homestead, Wynwood and Brickell (Wilke et al., 2019c). Data collected from mosquito traps represent a random sampling from the actual mosquito population, and have served as the major indicator for the evaluation of vector control efficacy for years (Pruszynski et al., 2017; Williams et al., 2022). However, due to various unexpected reasons such as loose or torn

* Corresponding author.
E-mail address: ruan@math.miami.edu (S. Ruan).
[1] Contributed equally to this work.

https://doi.org/10.1016/j.actatropica.2023.106837
Received 22 November 2022; Received in revised form 5 January 2023; Accepted 13 January 2023
Available online 16 January 2023

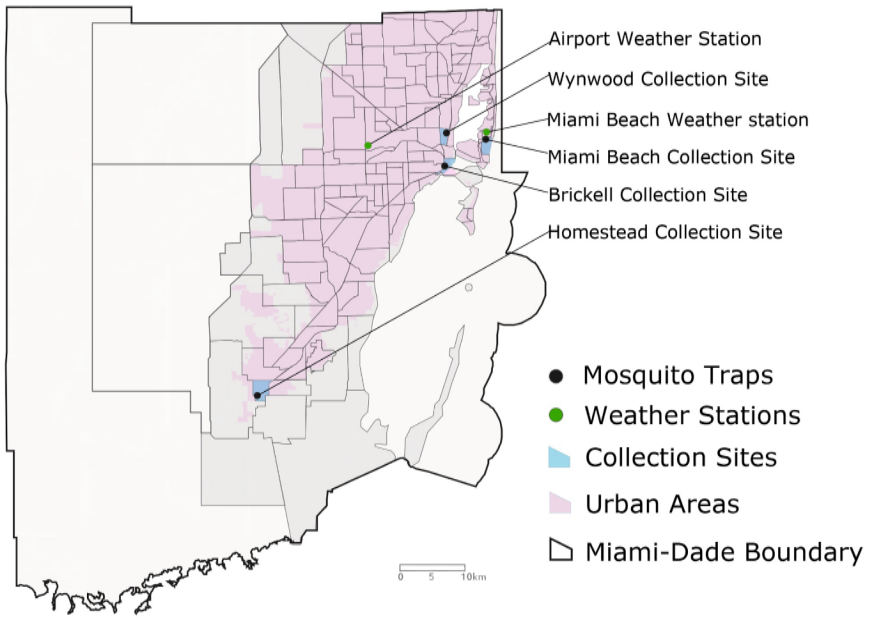

Fig. 1. Map of Miami-Dade County.

catch bags, locked gates, trap invasion by lizards, a certain number of traps occasionally malfunctioned, resulting in missing data from many observational days and traps (Stoddard, 2018). In addition, sometimes the functioning traps also fail to detect mosquitoes as they are not around due to environmental conditions (too cold, too hot, or too windy), not attracted by the traps, or their numbers are low for some unknown reason. As a result, over a three-year period, the traps located in Miami Beach, Homestead, Wynwood, and Brickell provide respectively 86, 109, 120, and 101 data points. Further, most of the data were not sampled on the same day, which makes it challenging to compare trap data from different locations via simple statistical methods. Thus the random sampling data may not directly provide credible estimations of the mosquito populations, which could pose difficulties in the assessment of vector control strategies. Mathematical models incorporated with mechanisms of population dynamics, when linked with trap data, are effective tools in understanding the underlying dynamics of the mosquito population and assessing the potential effectiveness of control interventions.

Mosquitoes are ectothermic, meaning that their reproduction, development, feeding, and survival rates rely on external sources of heat. The entomological parameters regarding mosquitoes' life cycle under different temperatures have been well studied and documented in many experimental papers (Delatte et al., 2009; Farnesi et al., 2009; Rueda et al., 1990; Yang et al., 2009). *Ae. aegypti* is known as "container-breeding", and female mosquitoes prefer to lay eggs in water-filled containers (Wilke et al., 2019b; 2020). Thus the abundance of *Ae. aegypti* may be influenced by rainfall, but its actual contribution is still unclear. Ordinary differential equation (ODE) models have been one of other significant approaches to simulate mosquito population dynamics, with the weather data incorporated as time-dependent parameters in the model systems. Models with human-mosquito interactions have been widely applied to explain the patterns of vector-borne disease outbreaks and estimate the potential future risks where the simulations were matched with human case data (Hladish et al., 2018; Metelmann et al., 2019; 2021; Poletti et al., 2011; Robert et al., 2016; Yé et al., 2007) or together with mosquito trap data (Caldwell et al., 2021; Leach et al., 2020; Li et al., 2019; Marini et al., 2017; Oidtman et al., 2021; Petrone et al., 2021; Yi et al., 2019). Specifically, to infer mosquito population in the field, differential equations models have been developed with variables representing the population in each stage of the mosquito's life cycle. Some models have been employed to calibrate the entomological parameters and the carrying capacity with climate data (Ewing et al., 2016; Ezanno et al., 2015; Simoy et al., 2015) and compare the model simulation with the seasonal trends indicated by trap data (Vaidya et al., 2014) or ovitrap data (Tran et al., 2013; 2020). Other models further include several uncertain factors subject to the natural environment, such as the influence of the intensity of rainfall on carrying capacity, the hazard risk of death in the wild, inter-specific competition, and the efficiency of traps or ovitraps (Erguler et al., 2016; Ewing et al., 2019; Lana et al., 2014; 2018; Marini et al., 2016; Nance et al., 2018; Valdez et al., 2018; White et al., 2011). Such assumptions result in unknown model parameters that need to be estimated via data fitting. The issue of parameter unidentifiability exists in most studies that involve data fitting, and this problem has been addressed in very few studies (Lana et al., 2014; 2018). On the basis of our search, only a few studies have investigated vector control strategies via simulations. Only one study provides results based on fitting to trap data (Cailly et al., 2012; Dumont and Chiroleu, 2010; White et al., 2011).

In this paper, we propose a deterministic model to investigate the growth, abundance, and control of *Ae. aegypti* mosquitoes in Miami-Dade County via the calibration of the *Ae. aegypti* trap data collected from January 2017 to December 2019 - which is a period not affected by the outbreaks of Zika in 2016 or COVID-19 after 2020. More specifically, we aim to (*i*) determine the model parameters that are identifiable and justify our findings via fitting experiments; (*ii*) investigate the necessity of incorporating temperature and precipitation data in the simulation of the local mosquito population dynamics by comparing the goodness of fitting; (*iii*) utilize the model to compare mosquito population and environmental differences among communities; and (*iv*) analyze the effectiveness of using insecticides under all possible situations.

2. Material and Methods

2.1. Data

Mosquito trap data. Each trap is turned on to attract and collect mosquitoes for precisely 24 hours on its surveillance day. Collected mosquitoes are identified to species. We therefore obtain the sampling of female *Ae. aegypti* captured in every single trap on each surveillance day. The trap attracts female mosquitoes by mimicking a host. Both males

Table 1
Goodness of Fitting

Quantity	Reduced Model	7-day Model	21-day Model	42-day Model
Miami Beach trap (86 data points)				
LOO	-342.20	-330.83	-328.84	-327.32
SE	41.72	39.54	38.80	38.36
Coverage	73	81	82	83
Homestead trap (109 data points)				
LOO	-671.17	-672.90	-676.05	-673.14
SE	127.48	130.93	130.62	128.59
Coverage	76	98	96	77
Wynwood trap (120 data points)				
LOO	-1029.69	-1011.86	-1014.99	-1020.23
SE	143.60	140.75	143.40	146.45
Coverage	56	91	94	90
Brickell trap (101 data points)				
LOO	-428.55	-424.19	-428.11	-430.18
SE	82.31	78.36	79.46	81.03
Coverage	90	96	97	96

LOO: leave-one-out cross-validation. SE: standard error. Coverage: number of points covered in the 95% prediction interval.

and females are collected by the traps but males are accidental catches since they were probably trying to mate with the females. Note that female *Ae. aegypti* only fly 100∼500 meters from their breeding sites, thus the trap count for each surveillance day can be regarded as a random sampling of the *Ae. aegypti* population in the corresponding community. In 2016 during the Zika outbreak, Miami-Dade County enforced intensive vector control activities, and the number of mosquitoes rapidly decreased. Since early 2020, COVID-19 pandemic has also brought influences on the frequency of outdoor activities and the exposure to mosquitoes, which could indirectly impact the *Ae. aegypti* population that primarily feed on human. Therefore, we focus our analyses on the trap data collected from January 2017 to December 2019 to avoid the unexpected influences of the two recent disease outbreaks. We select three traps located in Miami Beach, Wynwood, and Brickell, top-rated tourist destinations, thus possessing the highest human mobility. In addition, we select the trap located in Homestead, a populated residential area away from downtown Miami which has a more diverse environment compared to the other three. Fig. 1 illustrates all trap locations and the nearby weather stations.

Temperature and precipitation data. The daily average temperature and daily precipitation during the study period were obtained from the open-access database of the National Oceanic and Atmospheric Administration (NOAA). We choose data from the weather station that is geographically the closest to each trap location to represent the local community weather: data from Miami International Airport for traps in Brickell, Wynwood, and Homestead; and data from Miami Beach station for the trap in Miami Beach.

Thermal-response test data. We extract the entomological parameters of *Ae. aegypti* under various temperatures from published experiment data (Yang et al., 2009). Specifically, we collect the temperature-dependent data points on the average survival time for the aquatic phase, the average transition time from the aquatic stage to adult, the average survival time for female mosquitoes, and the average oviposition rate (*i.e.* the number of eggs laid per mosquito per day).

2.2. Baseline Model

We develop a deterministic ODE model with time-dependent parameters to simulate the *Ae. aegypti* population in each community. To incorporate the least number of unknown parameters, we simply subdivide the mosquito population into two classes: the immature mosquito population in the aquatic stage at time t ($J(t)$), and the adult female mosquito population at time t ($A(t)$). We only consider adult female *Ae. aegypti* because only female mosquitoes are seeking for blood meals and could be attracted to the traps. The compartmental model is presented in Fig. A1 and equations are given as follows:

$$\begin{aligned} J'(t) &= b(t)\left(1-\frac{J(t)}{K(t)}\right)A(t) - \mu_1(t)J(t) - d(t)J(t), \\ A'(t) &= \frac{1}{2}d(t)J(t) - \mu_2(t)A(t), \end{aligned} \tag{2.1}$$

where $b(t)$ represents the time-dependent oviposition rate, $d(t)$ denotes the time-dependent development rate, $\mu_1(t)$ and $\mu_2(t)$ respectively refer to the time-dependent death rates of immature and adult mosquitoes. The fraction $1/2$ in the second equation refers to our assumption that half of the immature population will develop into adult female mosquitoes. We assume that there is a carrying capacity for the aquatic stage population, $K(t)$, which may depend on time.

2.3. Entomological Parameters

The entomological parameters $b(t), d(t), \mu_1(t)$, and $\mu_2(t)$ are obtained by composing the time-dependent temperature function and the corresponding temperature-dependent entomological function. Let T denote the variable of temperature, we adopt the thermal-response functions as shown below (Mordecai et al., 2017).

$$\mu_1(T) = \frac{1}{c(T-T_0)(T_m-T)^{\frac{1}{2}}}, \tag{2.2}$$

$$\mu_2(T) = \frac{1}{c(T-T_0)(T_m-T)}, \tag{2.3}$$

$$b(T) = c(T-T_0)(T_m-T)^{\frac{1}{2}}, \tag{2.4}$$

where in each function, T_0 and T_m are the minimum and maximum temperature for the survival of *Ae. aegypti* at the corresponding stage, respectively, with c being a positive rate constant.

$$d(T) = \frac{aT_K e^{b(1/298.15 - 1/T_K)}}{298.15\left(1+e^{c(1/d-1/T_K)}\right)}, \tag{2.5}$$

where T_K is the temperature in Kelvin scale and a, b, c, d are positive constants. All coefficients shown in functions (2.2)-(2.5) are fitted to the thermal-response test data (Yang et al., 2009). The fittings are carried out by utilizing the method of Monte Carlo Markov Chain (MCMC) via the software *Stan*. The fitted coefficients for each function are summarized in Table 2, and the fitting outcomes together with the experimental data are plotted in Fig. 2. In this way, we obtain the entomological parameter values of *Ae. aegypti* under arbitrary temperature.

To obtain the time-dependent entomological parameters in model (2.1), we first acquire the daily temperature data T_i, with $i = 0, 1, 2, \ldots, N$ (N denotes the last day of simulation). By composing the temperature-dependent functions, we get the entomological values on each day, $\mu_1(T_i), \mu_2(T_i), b(T_i), d(T_i)$ with $i = 0, 1, 2, \ldots, N$. Finally, we fit each daily entomological data to trigonometric functions with a period of 365 days to get the continuous time dependent values: $\mu_1(t), \mu_2(t), b(t), d(t)$. The time-dependent entomological parameters are summarized in Table 3.

2.4. Assumptions on the Carrying Capacity

The carrying capacity for immature mosquito population could be directly impacted by the cumulative rainfall in the area. Water puddles and water-filled containers are perfect resources for *Ae. aegypti* to lay eggs, so cumulative rainfall may have a positive impact on the carrying capacity. We formulate

$$K(t) = K(1 + \alpha P_n(t)) \tag{2.6}$$

with K being the baseline carrying capacity, and α being the impact intensity of rainfall on carrying capacity. $P_n(t)$ is an index that measures the effect of cumulative rainfall in the past n days at time t, and is

Table 2
Thermal-response Functions with Fitted Coefficients

Variables	Functions	Estimates (median and credible interval)			
$\mu_1(T)$	$\frac{1}{c(T-T_0)(T_m-T)^{\frac{1}{2}}}$	c	T_0	T_m	
		0.0254	2.3209	31.0033	
		(0.0012, 0.0397)	(0.0002,7.1740)	(30,3400.6216)	
$\mu_2(T)$	$\frac{1}{c(T-T_0)(T_m-T)}$	c	T_0	T_m	
		0.1037	6.4429	41.4382	
		(0.0561,0.1039)	(2.8497, 9.0406)	(37.6608,47.1059)	
$b(T)$	$\frac{1}{cT(T-T_0)(T_m-T)^{\frac{1}{2}}}$	c	T_0	T_m	
		0.0058	14.0343	39.0899	
		(0.0022,0.0103)	(8.0104,18.6666)	(34.4189,51.9590)	
$d(T)$	$\frac{aT_K e^{b(1/298.15-1/T_K)}}{298.15(1+e^{c(1/d-1/T_K)})}$	a	b	c	d
		0.1666	21388	32013	300.02
		(0.1164,0.2000)	(21629,47348)	(21629,47348)	(299.67,300.38)

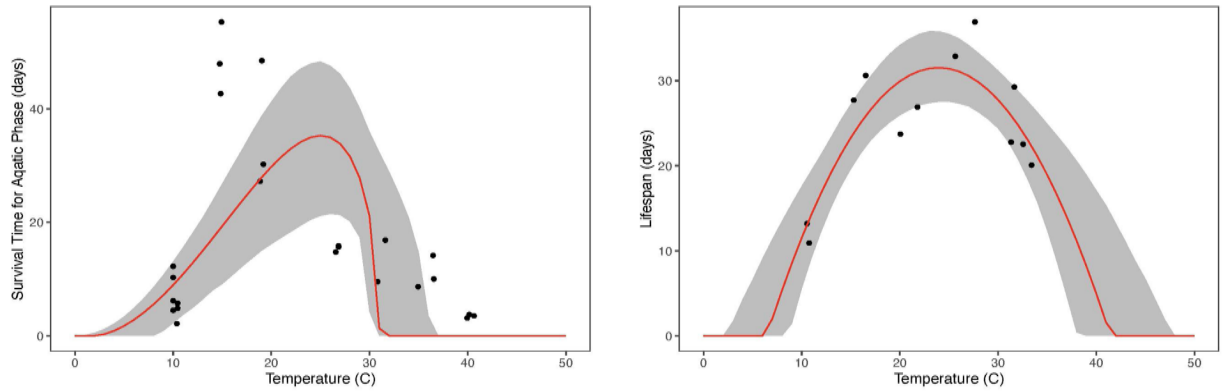

(a) $1/\mu_1(T)$: Lifespan of juvenile. (b) $1/\mu_2(T)$: Lifespan of adult.

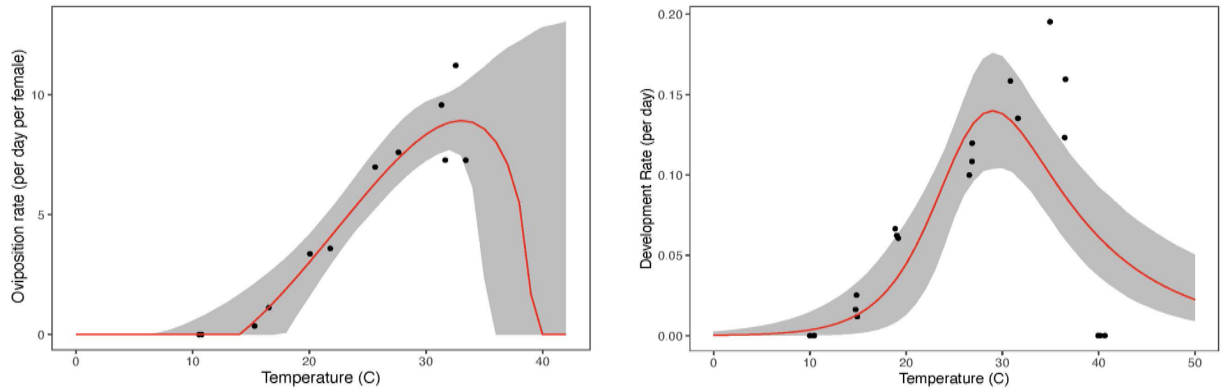

(c) $b(T)$: Birth rate. (d) $d(T)$: Developmental rate.

Fig. 2. Temperature-dependent entomological parameters. The thermal-response functions are fitted to the experimental data obtained from (Yang et al., 2009). In each figure, the dots represent experimental data, the red curve represent the best-fit function, and the gray area represent the 95% credible interval (CI).

formulated so that $0 \le P_n(t) \le 1$ for all $t \ge 0$. To determine this index, we calculate the n-day cumulative rainfall and get the time sequence data $\{C_n(T_i)\}$, $i = 1, 2, 3, \ldots, N$. Select the highest 2.5% quantile cumulative rainfall value and denote it as $C^n_{\max}$, and define

$$P_n(T_i) = \begin{cases} C_n(T_i)/C^n_{\max}, & \text{if } C_n(T_i) < C^n_{\max}, \\ 0, & \text{if } C_n(T_i) \ge C^n_{\max} \end{cases}$$

for each day $i = 0, 1, 2, \ldots, N$ in the study period. The reason for defining $P_n(T_i) = 0$ for those days with excessive rainfall is to account for flushing of breeding sites resulting from such extreme events. We then fit the data set $P_n(T_i)$ with $i = 0, 1, 2, \ldots, N$ to trigonometric functions to obtain the continuous-time precipitation index function $P_n(t)$. The time-dependent precipitation parameters are summarized in Table 3.

On one hand, the duration of *Ae. aegypti* maturation cycle (that is, the period for eggs to develop into adults) is approximately 14 days, thus the rainfall accumulated in the past 14 or more days could impact resources available for the current generation of immature mosquitoes. On the other hand, small-size water puddles would diminish in several days without continuous rainfall, so precipitation might not have a long-time impact on such breeding sites. Therefore, to examine in which accumulation fashion the rainfall is impacting local *Ae. aegypti* population, we propose four different assumptions on the carrying capacity: **Reduced Model** assumes a constant baseline carrying capacity, **7-day Model, 21-day Model**, and **42-day Model** respectively assumes rainfall accumulated in the past 7, 21, and 42 days would impact the carrying

Table 3
Time-dependent Model Parameters

Miami International Airport Weather Station	
$\mu_1(t)$ - death rate for juvenile	$0.03411272 - 0.00299637\sin(2\pi t/365) - 0.00350181\cos(2\pi t/365)$
$\mu_2(t)$ - death rate for adult	$0.03354552 - 0.00073822\sin(2\pi t/365) - 0.00050008\cos(2\pi t/365)$
$b(t)$ - birth rate	$6.20618176 - 0.96169481\sin(2\pi t/365) - 1.85341518\cos(2\pi t/365)$
$d(t)$ - development rate	$0.11026478 - 0.01650584\sin(2\pi t/365) - 0.03270561\cos(2\pi t/365)$
$P_7(t)$ - 7-day precipitation index	$0.20877977 - 0.05637451\sin(2\pi t/365) - 0.14470886\cos(2\pi t/365)$
$P_{21}(t)$ - 21-day precipitation index	$0.28119345 - 0.11241392\sin(2\pi t/365) - 0.20581943\cos(2\pi t/365)$
$P_{42}(t)$ - 42-day precipitation index	$0.34709785 - 0.17999706\sin(2\pi t/365) - 0.23746802\cos(2\pi t/365)$
Miami Beach Weather Station	
$\mu_1(t)$ - death rate for juvenile	$0.03309639 - 0.00045398\sin(2\pi t/365) - 0.00083619\cos(2\pi t/365)$
$\mu_2(t)$ - death rate for adult	$0.0335949 - 0.00039216\sin(2\pi t/365) + 0.000011939\cos(2\pi t/365)$
$b(t)$ - birth rate	$5.8358171 + 0.36835033\sin(2\pi t/365) - 2.04066277\cos(2\pi t/365)$
$d(t)$ - development rate	$0.10413367 + 0.00644022\sin(2\pi t/365) - 0.03762437\cos(2\pi t/365)$
$P_7(t)$ - 7-day precipitation index	$0.19671585 - 0.02564263\sin(2\pi t/365) - 0.0678024\cos(2\pi t/365)$
$P_{21}(t)$ - 21-day precipitation index	$0.27737096 - 0.01935936\sin(2\pi t/365) - 0.0982553\cos(2\pi t/365)$
$P_{42}(t)$ - 42-day precipitation index	$0.37260115 - 0.02072676\sin(2\pi t/365) - 0.13756741\cos(2\pi t/365)$

capacity.

$$\begin{aligned} K(t) &= K, \qquad (\text{ReducedModel}) \\ K(t) &= K(1+\alpha P_7(t)), \qquad (7-\text{dayModel}) \\ K(t) &= K(1+\alpha P_{21}(t)), \qquad (21-\text{dayModel}) \\ K(t) &= K(1+\alpha P_{42}(t)) \qquad (42-\text{dayModel}). \end{aligned}$$

2.5. Fitting

We use the MCMC method to fit the female adult *Ae. aegypti* count predicted by the model to the actual number of observed *Ae. aegypti* in each trap. Specifically, on each trap day, we assume that the actual mosquito count would follow a Poisson distribution with mean value proportional to the mosquito population predicted by the model for the whole community. Denote D_i as the trap count on day i, then

$$D_i \sim \text{Poisson}(q{\cdot}A(i)),$$

where q represents the trap efficiency in attracting *Ae. aegypti*. The expected trap count is proportional to the fraction of blood-seeking female adult mosquitoes and the trap's efficiency in catching such mosquitoes. Here we consider a combined effect of these two fractions and denote q as trap efficiency for simplicity.

The MCMC method samples the posterior distributions of model parameters by maximizing the likelihood function

$$\prod_{i \text{ for all trap days}} \frac{[qA(i)]^{D_i} e^{-qA(i)}}{D_i!}.$$

Based on all of our model assumptions, there are five unknown parameters for the **n-day Model** and four for the **Reduced Model**: (K, α, q, J_0, A_0), where J_0 and A_0 refer to the initial immature and mature *Ae. aegypti* population on the first simulation day, respectively.

2.6. Parameter Identifiability

We reparameterize the model to show that the baseline carrying capacity, K, cannot be identified based on trap data. Let $\widetilde{J}(t) = J(t)/K$ and $\widetilde{A}(t) = A(t)/K$. The model (2.1) becomes

$$\begin{aligned} \widetilde{J}'(t) &= b(t)\left(1 - \frac{\widetilde{J}(t)}{1+\alpha P_n(t)}\right)\widetilde{A}(t) - \mu_1(t)\widetilde{J}(t) - d(t)\widetilde{J}(t), \\ \widetilde{A}'(t) &= \frac{1}{2}d(t)\widetilde{J}(t) - \mu_2(t)\widetilde{A}(t) \end{aligned}$$

with initial conditions $\widetilde{J}(0) = J_0/K$ and $\widetilde{A}(0) = A_0/K$. The trap data then follows a Poisson distribution with respect to the new variable $\widetilde{A}(t)$:

$$D_i \sim \text{Poisson}(q{\cdot}K{\cdot}\widetilde{A}(i)).$$

Thus, in the reparameterized system the carrying capacity K only impacts the dynamics as in terms $J_0/K, A_0/K$, and $q{\cdot}K$, which are coupled with parameters (q, J_0, A_0). Therefore, one will only identify parameters $(\alpha, qK, J_0/K, A_0/K)$ via fitting, and the parameter K is theoretically unidentifiable.

Additionally, we conduct fitting experiments with synthetic data to show the practical identifiability of the model parameters. The experiments and results of the practical identifiability are summarized in Figs. A2–A4.

2.6.1. Model Comparison

We now fit each model to the real trap data (specified in section 2.1) while fixating the carrying capacity $K = 1,000$ and the initial date of simulation as January 1st, 2017. In each fitting, we sample a total of four independent chains that the first 2,000 iterations as burn-in, where in each chain we discard all but every second sampled value to obtain 4,000 sampled values. Convergence was checked by calculating the $\widehat{R}$ value in Gelman-Rubin diagnostic (Gelman and Rubin, 1992) and examining the effective sample size.

We compare the goodness of fit among all four models by evaluating the leave-one-out cross-validation (LOO). The calculations are performed via the *Python* package *ArviZ* which conducts an efficient computation of LOO from MCMC samples (Vehtari et al., 2017; 2015). Table 1 shows the model comparison results for the fittings of all four traps.

1. The differences of LOO values among all four models are far smaller than the scale of standard errors. This indicates that all models perform equivalently well in fitting the trap data.
2. The **7-day Model** and **21-day Model** tend to cover more data points in their 95% prediction intervals.

From a statistical point of view, there is no significant difference in the goodness of fitting for all models. However, the prediction intervals of models incorporated with precipitation data can include the majority of trap data under all scenarios investigated. Therefore, **7-day Model** and **21-day Model** show a slightly better fitting will be used to explore our following questions.

2.6.2. The Combined Trap Model

We now extend the **n-day Model** for the simulation of mosquito population in four locations. By assuming that all traps share the same efficiency, we can use this model to compare the mosquito abundance and rainfall dependency among communities. Specifically, we consider four traps and denote $J_i(t)$ and $A_i(t)$ as the juvenile and female adult population in trap i ($i = 1, 2, 3, 4$) at time t, and have the following **Combined Trap Model** with n-day cumulative rainfall data $P_n^i(t)$ for each trap location:

$$\begin{aligned} J_i'(t) &= b^i(t)\left(1 - \frac{J_i(t)}{K_i(1+\alpha_i P_n^i(t))}\right)A_i(t) - \mu_1^i(t)J_i(t) - d^i(t)J_i(t), \\ A_i'(t) &= \frac{1}{2}d^i(t)J_i(t) - \mu_2^i(t)A_i(t), \text{ for } i = 1,2,3,4. \end{aligned} \tag{2.7}$$

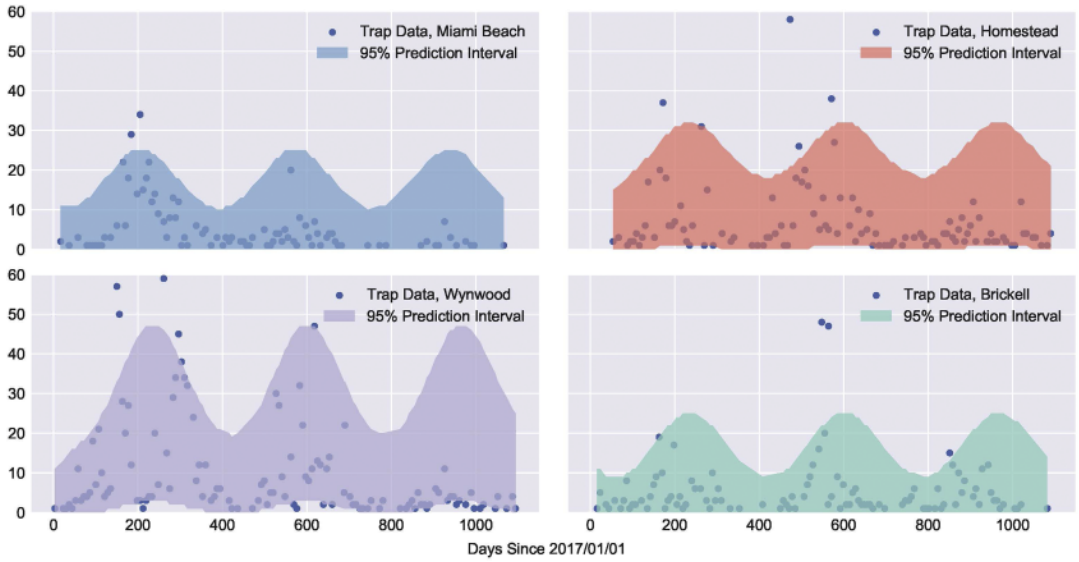

(a) Fitting outcome for traps in Miami Beach, Homestead, Wynwood, and Brickell.

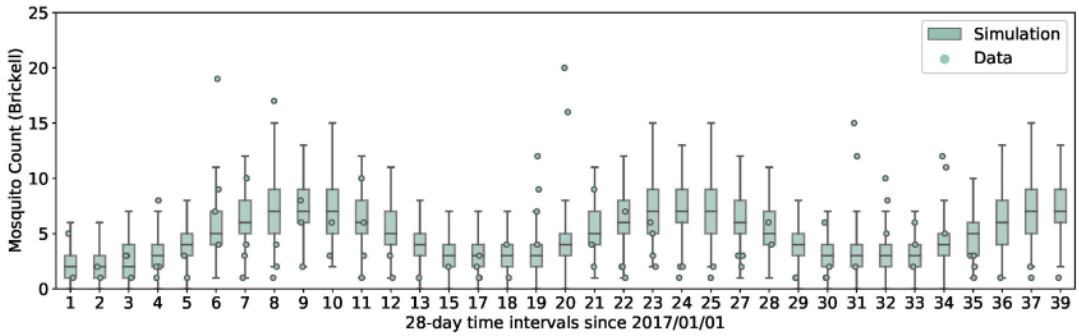

(b) Fitting outcome for the trap in Brickell on a 28-day basis.

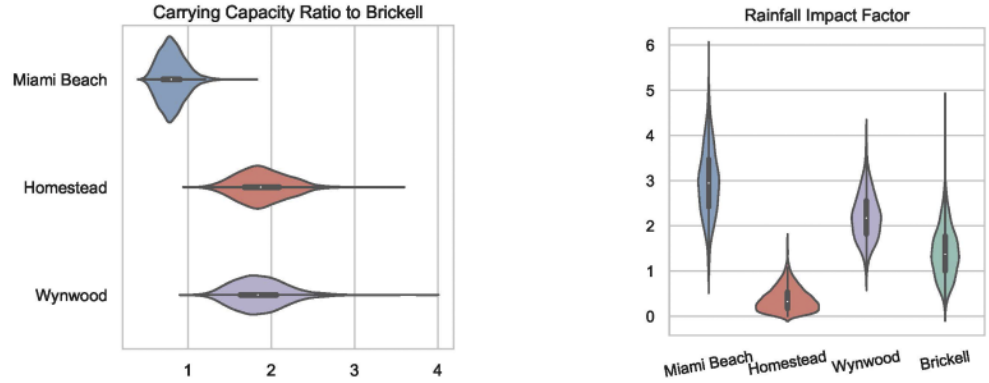

(c) Posterior distribution of carrying capacities. (d) Posterior distribution of rainfall impact factor.

Fig. 3. Fitting outcomes of the Combined Trap Model with 21-day cumulative rainfall. (*a*) The colored bands indicate that the trap count of *Ae. aegypti* obtained on each trap day should lie within the band with a 95% probability. (*b*) Each box with and whiskers show the median, interquartile range, and 95% CIs of predicted trap counts derived from simulations based on 100 parameter combinations drawn from the posterior distributions. (*c*)&(*d*) Each violin plot represents the posterior distribution of the corresponding parameter. In a violin plot: the white dot represents the median; the thick black bar represents the interquartile range; the thin black bar represents the rest of the distribution; the two colored sides represent the shape of the distribution (wider sides indicate higher probability).

Note that the entomological parameters $b^i(t), d^i(t), \mu_1^i(t), \mu_2^i(t)$ could also differ among traps due to different local temperature profiles. Denote D_i^j as the trap count on day i in trap j, then

$$D_i^j \sim \text{Poisson}\big(q \cdot A_j(i)\big).$$

And the MCMC method will sample the posterior distributions of parameters that maximize the likelihood function:

$$\prod_{j=1,2,3,4} \prod_{\substack{i \text{ in all days} \\ \text{of trap } j}} \frac{\left[qA_j(i)\right]^{D_i^j} e^{-qA_j(i)}}{D_i^j!}.$$

There are a total of 17 unknown parameters: the carrying capacity in

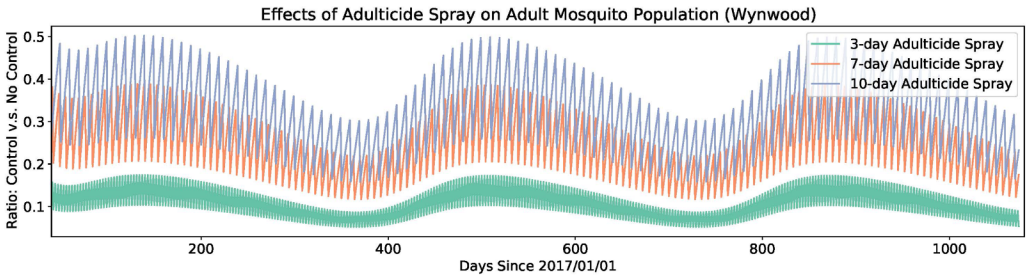

(a) Effects of adulticide on adult population.

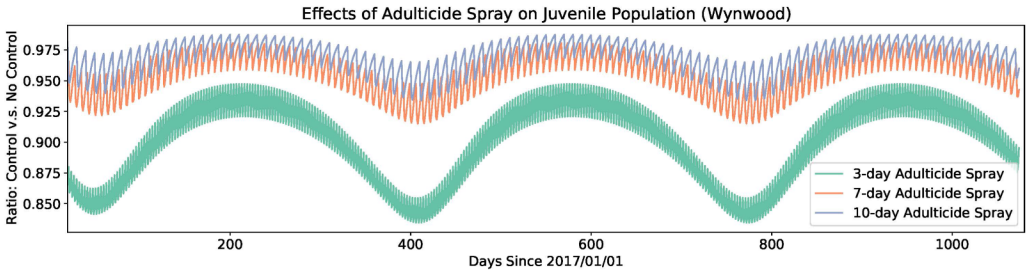

(b) Effects of adulticide on juvenile population.

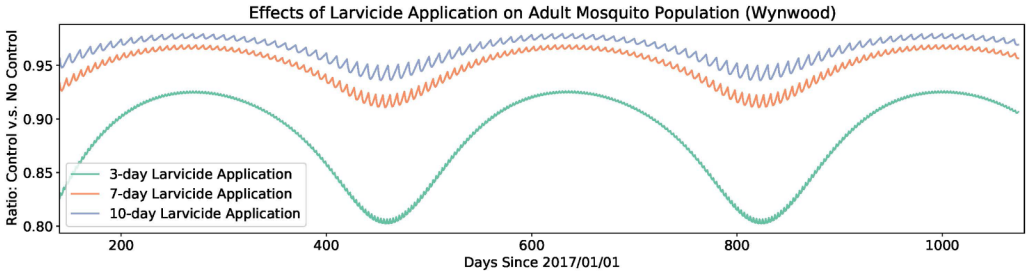

(c) Effects of larvicide on adult population.

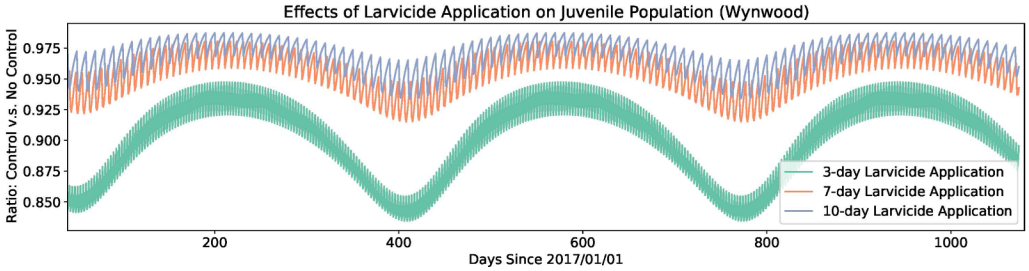

(d) Effects of larvicide on juvenile population.

Fig. 4. Effects of adulticide and larvicide in Wynwood. Effects are measured by calculating the daily fraction between mosquito population with and without control.

each trap K_i, the rainfall impact factor for each trap location α_i, initial juvenile population $J_i(0)$, initial female adult population $A_i(0)$, and trap efficiency q. Similar to the analysis of the single trap model (2.1), it is easy to see that one has to presume the carrying capacity in one of the traps to identify other parameters. First we can fix the carrying capacity of trap 1 as $K_1 = K$ with K being a baseline value. Then we fit the above model to data from four traps with the aim of estimating a total of 16 unknowns: $K_2/K, K_3/K$ and K_4/K as relative carrying capacity ratios, the rainfall impact factors α_i, the relative initial populations $J_i(0)\ /K$ and $A_i(0)/K$ $(i = 1, 2, 3, 4)$, and $q{\cdot}K$. The posterior distributions of $K_2\ /K, K_3\ /K$ and K_4/K could help compare the *Ae. aegypti* population among different areas, and the estimated values of α_i could help evaluate the dependency of the mosquito population on rainfall in each community.

We conduct similar synthetic tests to confirm that all parameters are identifiable and the parameter estimations are not affected by the presumed baseline carrying capacity K for trap 1. Then we take $K = 1000$ as the carrying capacity for the Brickell trap, and fit model (2.7) with $n = 7$ and $n = 21$ to the trap data in Brickell, Wynwood, Miami Beach, and Homestead. The fitting outcomes are discussed in the following section, and the posterior distribution of all parameters being estimated are adopted to generate further simulations on insecticide applications.

3. Results

3.1. Mosquito Abundance and Rainfall Impact Comparison

Due to personnel shortages, the schedule and frequency of trap counts differ from community to community. Thus one cannot directly compare the abundance of *Ae. aegypti* among the four communities. The average trap count of *Ae. aegypti* per trap day in Brickell, Homestead, Wynwood, and Miami Beach are 5.25, 7.36, 10.91, and 5.22. It is insufficient to conclude the lower abundance of *Ae. aegypti* in Brickell and Miami Beach comparing to the other two communities because the trap capture could undoubtedly be affected by randomness. Here we

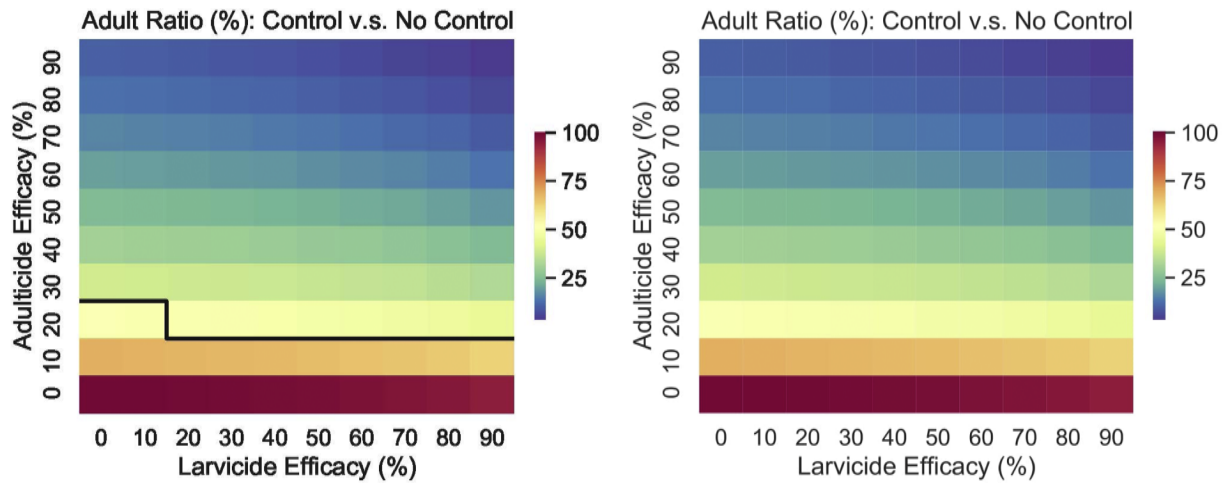

(a) Same-day application. (b) Alternating application.

Fig. 5. Combined use of adulticide and larvicide on 7-day schedule.

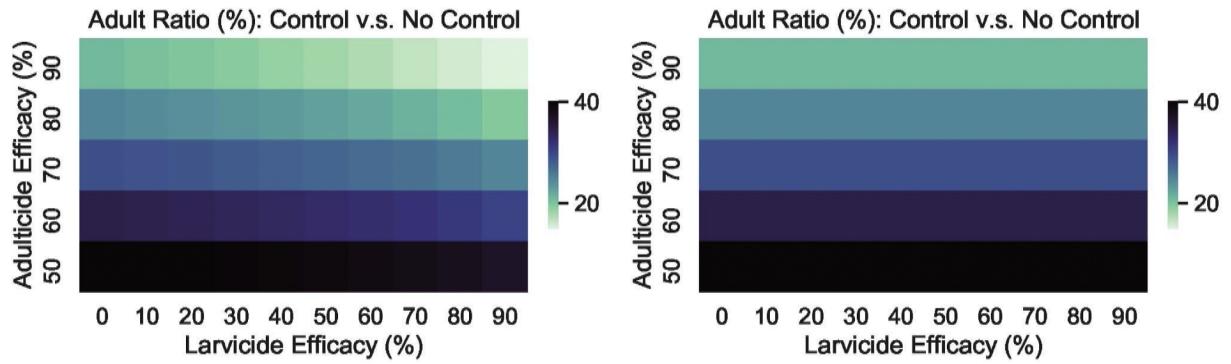

(a) Same-day application. (b) Alternating application.

Fig. 6. Combined use of adulticide and larvicide on 14-day schedule.

utilize our model to compare the mosquito population among communities, and in order to do this, we assume that the trap efficiency in attracting and trapping *Ae. aegypti* is the same among all four communities.

The fitting outcomes for real trap data with 21-day cumulative rainfall are presented in Fig. 3: (*a*) shows that the model can explain the trap counts in all four communities, (*b*) visualizes how data points fall into the prediction interval on a monthly basis (with results for the other three traps in Fig. A5), (*c*) shows the estimation of relative carrying capacities (thus abundance) among the communities, and (*d*) shows the posterior distributions of the rainfall impact factor in different communities. Corresponding results obtained from the Combined Trap Model with 7-day cumulative rainfall are summarized in Fig. A6 with consistent conclusions as summarized below.

Mosquito Abundance. From the posterior distribution of carrying capacity ratios we know that Brickell and Miami Beach tend to have less *Ae. aegypti* population than Homestead and Wynwood. Thus the extremely high trap count in Miami Beach in summer 2017 could be caused either by temporally high adult *Ae. aegypti* population or by the randomness of sampling. Such a high count was not observed continuously in the latter part of the study period. Then based on our mechanistic-based model, the tentative high trap counts in Miami Beach do not link to high local mosquito abundance.

Rainfall Impact. The rainfall impact factor value for each trap (α_i) measures how the fluctuation of precipitation may affect the overall carrying capacity in the surrounding area. Our results show that the trap in Homestead, the only residential place among all four locations, has the lowest rainfall impact factor. Thus cumulative rainfall may affect the breeding sites of *Ae. aegypti* more significantly in the tourist areas where the small water containers are usually left unattended.

3.2. Effects of Vector Control

Mosquito control interventions in Miami-Dade County are conducted on a two-week basis by applying insecticides mainly via truck spray Miami Dade County Mosquito Control. The aerial spray of adulticide kills flying mosquitoes upon contact and lasts only a short period of time, then degrades into harmless byproducts. Larviciding prevents immature

mosquitoes from completing their immature stage and developing into biting mosquitoes. The most frequently used larvicide in the County, *Bacillus thuringiensis israelensis* (*Bti*) (Wilke et al., 2021b), can be applied either by hand or truck spray to areas of standing water as potential mosquito breeding sites.

Here we utilize our well-calibrated model to simulate vector control strategies with insecticide efficacy ranging from widely assumed intervals. We assume the efficacy of adulticide as $\varepsilon_a \in [0,90]$, which means that adulticide can kill a percentage ε_a of adult mosquitoes upon contact. The application of adulticide is modeled by resetting the number of female adult mosquito population $A(t)$ on the application day t to $(1 - \varepsilon_a/100)A(t)$. The larvicide efficacy is denoted as $\varepsilon_l \in [0, 90]$, which means that larvicide can kill ε_l percent of the immature mosquito population over a 24-hour period. Then the first-day killing rate of juvenile can be parameterized as $\gamma = -\ln(1 - \varepsilon_l/100)$. Since larvicide is applied to water resources which could last and maintain its efficacy longer, we assume that the toxicity would decay exponentially at a rate of ν. While the half-life of *Bti* in soil could be long, studies found only 41% of the toxin would remain after 24 hours in water (Perez et al., 2015). Thus we model the time-dependent larvicide killing rate as $\gamma(0.41)^{\Delta t}$, where Δt measures the difference between current time and the last larvicide application time. We obtain the effectiveness of vector control strategies based on simulations with the fitted Combined Trap Model with 21-day cumulative rainfall, and similar conclusions are observed for the model with 7-day cumulative rainfall.

Effects of adulticide spray. We utilize the calibrated model for Wynwood to perform simulations on adulticide application under three different schedules: 3-day schedule (adulticide spray for every three days), 7-day schedule, and 10-day schedule. Fig. 4(a)-(b) show the effects of various schedules in comparison to no control given a 50% efficacy adulticide. All spraying schedules are effective in reducing the overall prevalence of the female adult population (Fig. 4(a)), hence should reduce the trap observations. In addition, the reduction of female adult mosquitoes would lead to decreased egg-laying rate hence a lower immature population. The most frequent 3-day spray schedule is the most effective strategy in reducing the adult mosquito population and also reduces the immature population by more than 10% (Fig. 4(b)).

Effects of larvicide application. Our simulations show that applying larvicides with 90% efficacy (Pruszynski et al., 2017) could reduce female adult mosquitoes by $10 \sim 20\%$ (Fig. 4(c)). In comparison to the 50% adulticide spray, larvicide is not as effective as adulticide in reducing mosquito population. Larvicide could kill a significant amount of the immature population during the application period. However, given the high prevalence of female adult mosquitoes, the immature population can be instantly compensated with newly laid eggs. Overall, the immature population could be maintained at a reasonably lower level, and the lower development rate leads to a reduced adult population.

Effects of combined application of adulticide and larvicide. We simulate the implementation of both adulticide and larvicide in a 7-day schedule under variously assumed insecticide efficacies. Fig. 5(a) shows the outcomes of such a 7-day control strategy where the adulticide and larvicide are applied on the same day. Under all possible efficacies, using larvicide alone would not reduce the female adult population by more than 6%, and the optimal control strategy is to use a combination of both insecticides. To reduce the female population by 50%, we need an insecticide combination with efficacies falling in the upper area segregated by the black border in Fig. 5(a).

Same-day versus alternating schedule. The Mosquito Control Department of Miami-Dade County conducts a two-week vector control strategy. The schedule of adulticide spray and larvicide application in the same area may not fall on the same day due to the availability of personnel. Then it is natural to ask about the necessity of implementing the two insecticides on a same-day schedule. We, therefore, conduct experiments for a 7-day and a 14-day control schedules where the insecticides are used either on the same day or alternatively (Fig. 5(b) and Fig. 6). We conclude that the alternating schedule possesses similar effectiveness in a high-frequency control program but could bring zero effect in larvicide application in a low-frequency program such as the one employed in Miami-Dade County. This finding coincides with the conclusion of the field study conducted by our ecology team (Wilke et al., 2021b), where the same-day application of both insecticides was superior to the alternating schedule.

4. Discussion

In this study, we utilized a deterministic model to fit the *Ae. aegypti* trap count data from four communities in Miami-Dade County over a three-year period. The time-dependent model parameters were obtained by combining the local temperature data and the temperature-dependent entomological data for *Ae. aegypti*. We found that the baseline carrying capacity and trap efficiency are two coupled parameters that cannot be separately identified based on trap data. We formulated four hypotheses about the impact of rainfall on the carrying capacity of *Ae. aegypti*, and found no statistical differences among the fitness of models. This means the **Reduced Model** without rainfall could also fit the *Ae. aegypti* trap count as well as the others under a statistical point of view. However, we would like to emphasize that this finding does not suggest limited impact of rainfall on *Ae. aegypti* population. The temperature and precipitation patterns are practically synchronized in South Florida, which makes the entomological parameters driven by temperature oscillations in our models sufficient to capture the trap count trends. For study sites with distinctive temperature and precipitation patterns, incorporating rainfall impact could become essential in the interpretation of *Ae. aegypti* population dynamics.

We applied the model to fit the trap count data collected from four communities. This allows us to compare the relative scale of *Ae. aegypti* population and the breeding site dependency on rainfall among different urban built environments. Wynwood, which is undergoing an intense gentrification process, and Homestead, which is undergoing an urbanization process, showed a relatively high *Ae. aegypti* abundance. Brickell, as a highly urbanized and high-income area with a high human population density but fewer aquatic habitats due to the absence of highly productive urban environments for mosquito development and proliferation, had a relatively low carrying capacity of *Ae. aegypti*. Miami Beach was the most affected area by the Zika virus in 2016. As a result of an intense joint effort made by the community and the Miami-Dade Mosquito Control Division, many important aquatic habitats were removed from the area and therefore the abundance of *Ae. aegypti* was impacted. Among all four investigated areas, we found that the breeding sites for *Ae. aegypti* in Homestead do not depend significantly on the cumulative rainfall. Thus reducing unattended artificial containers could help reduce the breeding sites of *Ae. aegypti* in rainy seasons and further help reduce the *Ae. aegypti* population.

In real practice, the success of adulticide spray also depends on many other aspects such as the specific time and location of the spray, wind, and precipitation (Stoddard, 2018), thus the practical adulticide efficacy

could be considerably lower than expected. Therefore, the dominant adulticide effect found in our simulation does not rule out the necessity of the integrated vector control strategy with both insecticides. Our finding on larvicide effectiveness is based on the assumption of applying larvicide in water where 41% of the toxin remained after one day. However, the half-life of *Bti* is a lot longer in soil, and plant surface (Perez et al., 2015), and field studies showed that aerial larvicide application could significantly reduce the trap count of adult mosquitoes. Therefore, the half-life of *Bti* could be considerably different in diversified urban environments and the effectiveness of larvicide application could be underestimated in the simulations presented herein.

CRediT authorship contribution statement

Jing Chen: Methodology, Formal analysis, Investigation, Writing – original draft, Writing – review & editing. **Xi Huo:** Methodology, Formal analysis, Investigation, Writing – original draft, Writing – review & editing. **André B.B. Wilke:** Data curation, Writing – review & editing. **John C. Beier:** Writing – review & editing. **Chalmers Vasquez:** Data curation, Writing – review & editing. **William Petrie:** Data curation, Writing – review & editing. **Robert Stephen Cantrell:** Writing – review & editing. **Chris Cosner:** Writing – review & editing. **Shigui Ruan:** Methodology, Formal analysis, Writing – review & editing.

Declaration of Competing Interest

The authors declare that there is no conflict of interest.

Data availability

Data will be made available on request.

Acknowledgement

This research was partially supported by the National Science Foundation (DMS-1853622, DMS-1853562), the Miami-Dade Mosquito Control Division, and the CDC (https://www.cdc.gov/) grant 1U01CK000510-05: Southeastern Regional Center of Excellence in Vector-Borne Diseases: The Gateway Program. NSF and CDC had no role in the design of the study and collection, analysis, and interpretation of data and in writing the manuscript. The authors would like to thank the two anonymous reviewers for their helpful comments and valuable suggestions.

Appendix A. Practical Identifiability

A1. Single Trap Models

To validate our conclusions on parameter identifiability, we first run our model to generate synthetic data, then fit the identifiable model parameters to the data and compare the fitting outcomes with the actual parameter values being used.

Generate synthetic data. For each model, we first simulate the female adult population for a two-year time period by setting $J_0 = A_0 = K = 1000$, $\alpha = 1$, and $q = 5\%$, while adopting the local temperature and 7-day accumulated precipitation. Secondly, we randomly select 100 trap days and obtain the synthetic trap data on each corresponding day by drawing a sample from a Poisson distribution with mean value being the trap count predicted by the model.

Fitting experiments. To validate our conclusion that the carrying capacity K cannot be identified via fitting the models to the trap data, we conduct four fitting scenarios with various values of K being 500, 1000, 2000, and 5000. We utilize the package *Stan* for Bayesian inference to conduct all fittings via the MCMC methods.

As an example, we discuss our findings on the **7-day Model**, where we obtain similar conclusions for the **21-day Model** and **42-day Model**. The posterior distributions of the fitted parameters J_0/K, A_0/K, α, and $q{\cdot}K$ under all scenarios are pictured in Fig. A2 for the **7-day Model**. The fitting scenario with $K = 1000$ represents the case with the real carrying capacity, and the posterior distributions of all fitted parameters show that their fitted values are close to real values. Similar experiments are conducted for the **Reduced Model** with posterior distributions in Fig. A3 with consistent observations. Then we conclude from the synthetic tests that:

1. The actual carrying capacity K cannot be estimated from trap data.
2. Other parameters (J_0/K, A_0/K, α, $q{\cdot}K$) can be correctly identified.
3. The trap efficiency q cannot be identified as the carrying capacity is unidentifiable.

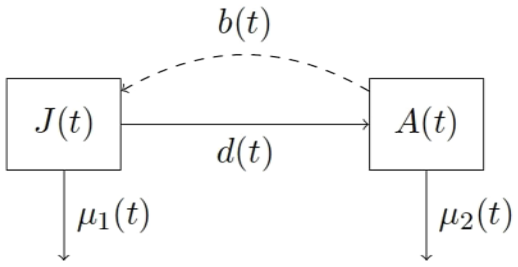

Fig. A1. Compartmental dynamics for *Ae. aegypti* population.

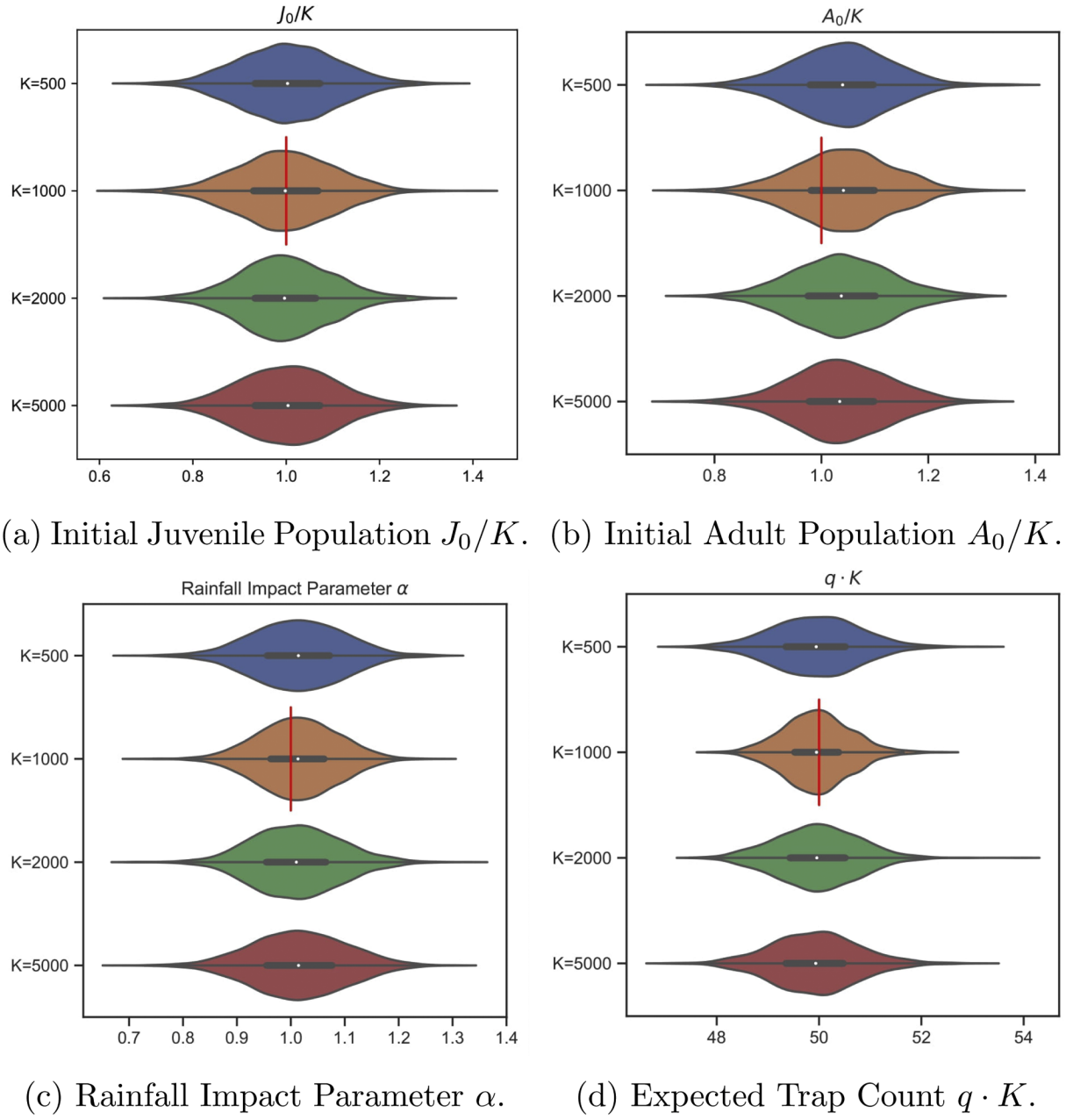

(a) Initial Juvenile Population J_0/K. (b) Initial Adult Population A_0/K.

(c) Rainfall Impact Parameter α. (d) Expected Trap Count $q \cdot K$.

Fig. A2. Fitting Validation for the **7-day Model**. Synthetic data were generated by letting $K = 1000$. Fitting were conducted under four scenarios by assuming $K = 500, 1000, 2000, 5000$. The figures show the posterior distributions of each model parameter under different assumed K values, where the red vertical bars represent the actual value of the model parameter used to generate synthetic data.

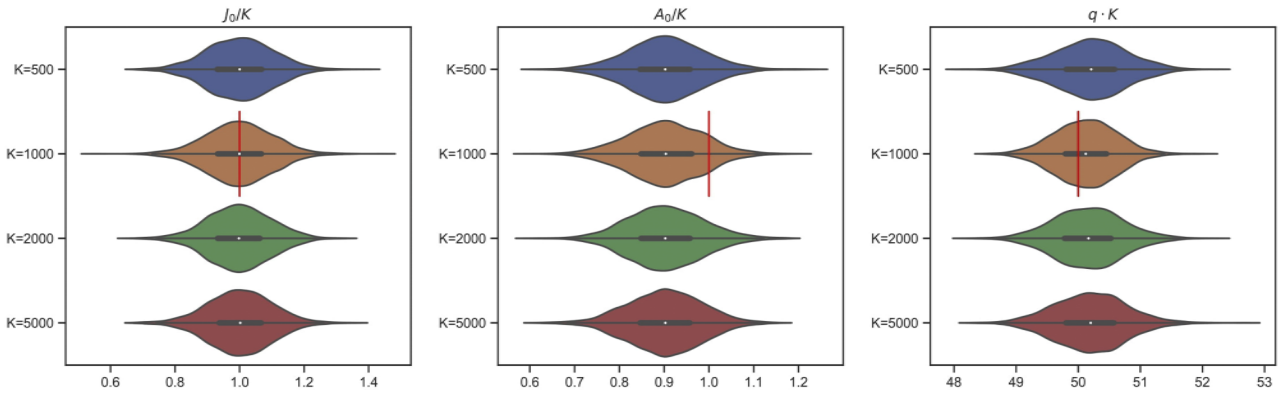

(a) Initial Juvenile J_0/K. (b) Initial Adult A_0/K. (c) Expected Trap Count $q \cdot K$.

Fig. A3. Fitting Validation for the **Reduced Model**. Synthetic data were generated by letting $K = 1000$. Fitting were conducted under four scenarios by assuming $K = 500, 1000, 2000, 5000$. The figures show the posterior distributions of each model parameter under different assumed K values, where the red vertical bars represent the actual value of the model parameter used to generate synthetic data.

A2. Combined Trap Model

We conduct similar synthetic test for the **Combined Trap Model** with outcomes shown in Fig. A4, and reach the conclusion in the main text.

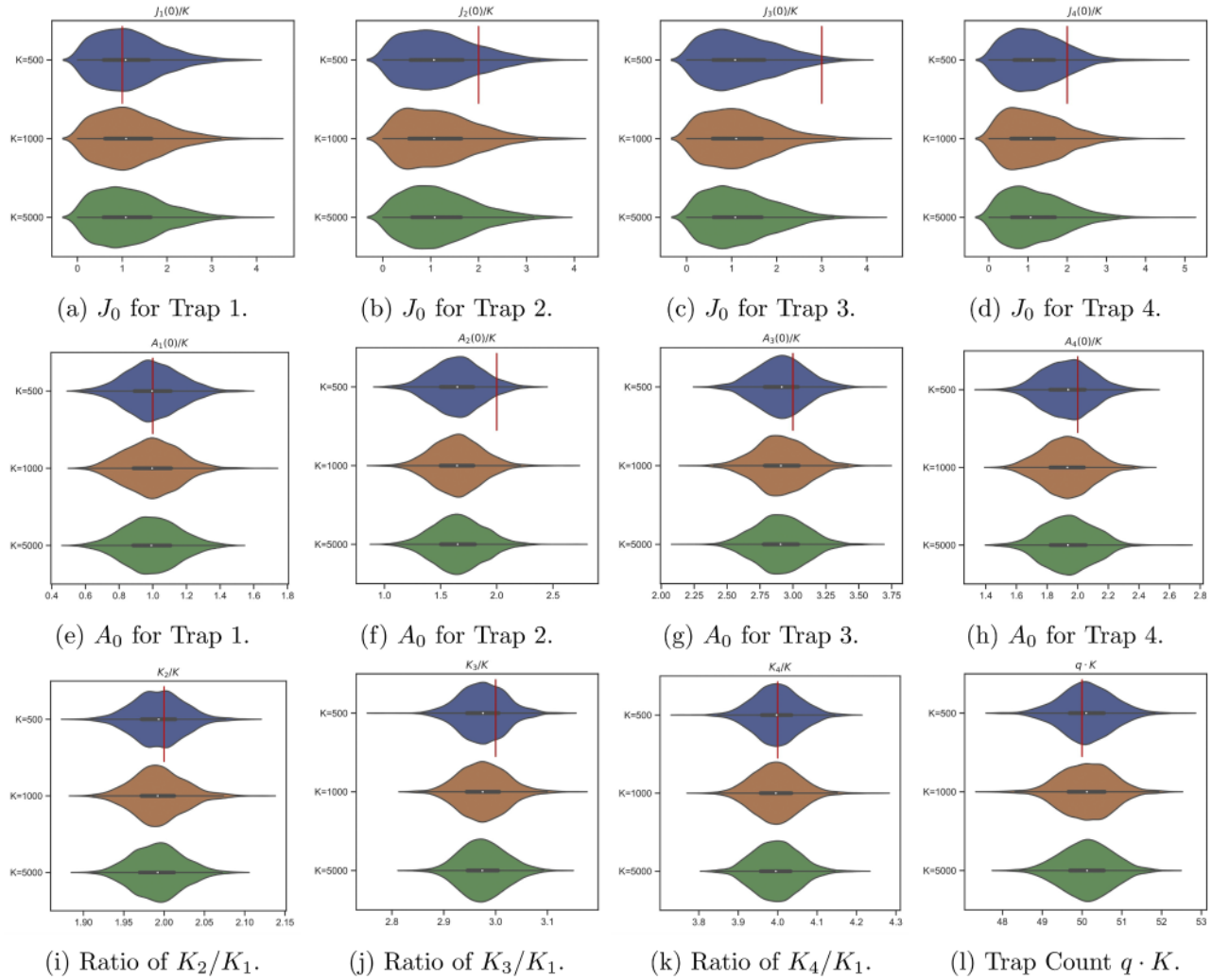

(a) J_0 for Trap 1. (b) J_0 for Trap 2. (c) J_0 for Trap 3. (d) J_0 for Trap 4.

(e) A_0 for Trap 1. (f) A_0 for Trap 2. (g) A_0 for Trap 3. (h) A_0 for Trap 4.

(i) Ratio of K_2/K_1. (j) Ratio of K_3/K_1. (k) Ratio of K_4/K_1. (l) Trap Count $q \cdot K$.

Fig. A4. Fitting Validation for the **Combined Trap Model**. Synthetic data were generated by setting the carrying capacity for Trap 1 as $K = 1000$. Fitting were conducted under four scenarios by assuming $K = 500, 1000, 5000$. The figures show the posterior distributions of each model parameter under different assumed K values, where the red vertical bars represent the actual value of the model parameter used to generate synthetic data.

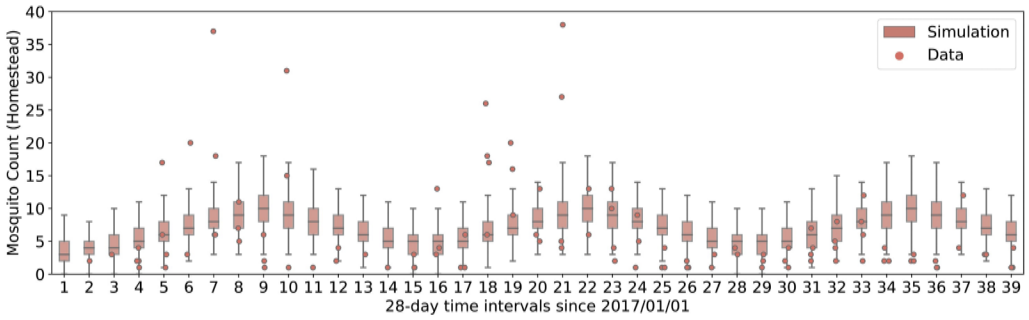

(a) Fitting Outcome for Trap in Homestead on a 28-day basis.

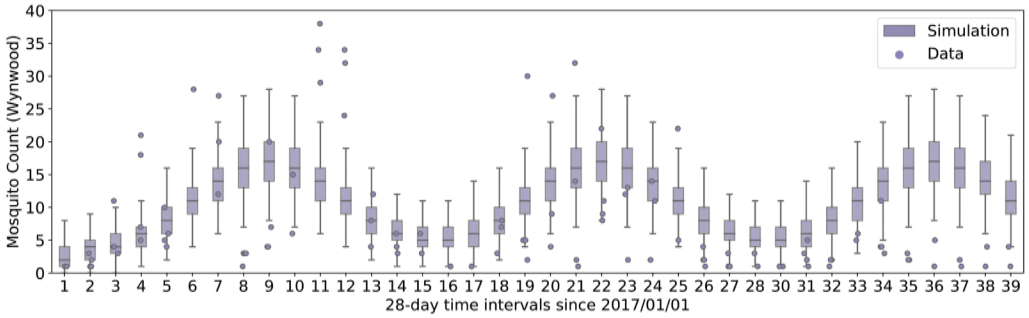

(b) Fitting Outcome for Trap in Wynwood on a 28-day basis.

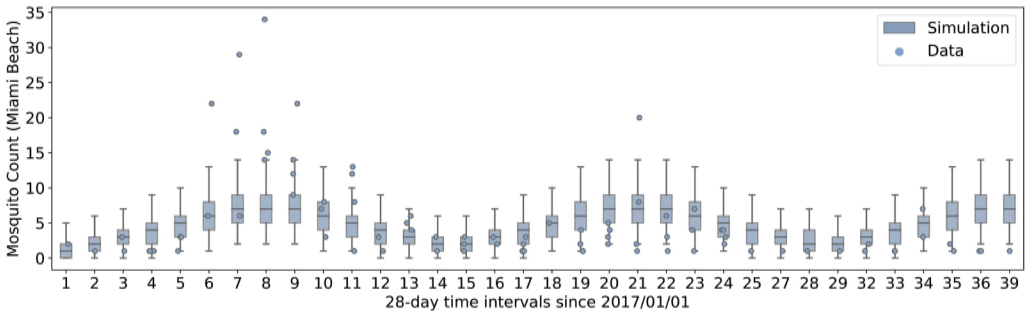

(c) Fitting Outcome for Trap in Miami Beach on a 28-day basis.

Fig. A5. Combined Fitting of Four Traps with 21-day cumulative rainfall.

(a) Fitting outcome for traps in Miami Beach, Homestead, Wynwood, and Brickell.

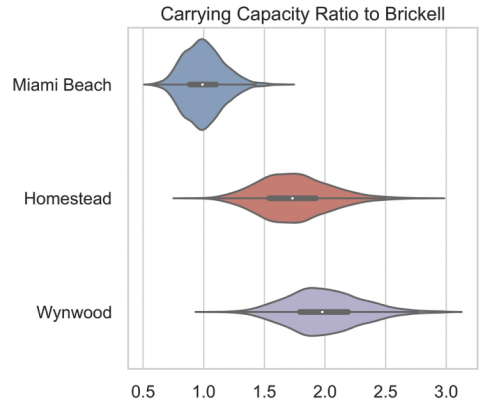

(b) Posterior distribution of carrying capacities.

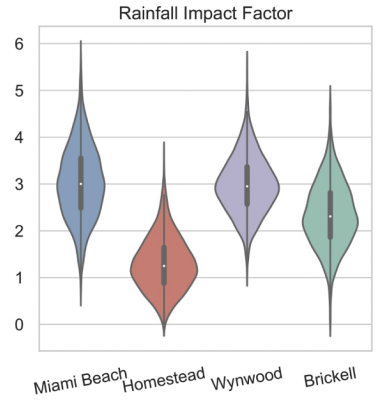

(c) Posterior distribution of rainfall impact factor.

Fig. A6. Fitting outcomes of the Combined Trap Model with 7-day cumulative rainfall.

References

Cailly, P., Tran, A., Balenghien, T., L'Ambert, G., Toty, C., Ezanno, P., 2012. A climate-driven abundance model to assess mosquito control strategies. Ecological Modelling 227, 7–17. https://doi.org/10.1016/j.ecolmodel.2011.10.027.

Caldwell, J.M., LaBeaud, A.D., Lambin, E.F., Stewart-Ibarra, A.M., Ndenga, B.A., Mutuku, F.M., Krystosik, A.R., Ayala, E.B., Anyamba, A., Borbor-Cordova, M.J., et al., 2021. Climate predicts geographic and temporal variation in mosquito-borne disease dynamics on two continents. Nature Communications 12 (1), 1–13.

Miami Dade County Mosquito Control,. https://www.miamidade.gov/global/solidwaste/mosquito/insecticides.page. Accessed: 2021-06-25.

Delatte, H., Gimonneau, G., Triboire, A., Fontenille, D., 2009. Influence of temperature on immature development, survival, longevity, fecundity, and gonotrophic cycles of aedes albopictus, vector of chikungunya and dengue in the indian ocean. Journal of Medical Entomology 46 (1), 33–41.

Dumont, Y., Chiroleu, F., 2010. Vector control for the chikungunya disease. Mathematical Biosciences and Engineering 7 (2), 313–345.

Erguler, K., Smith-Unna, S.E., Waldock, J., Proestos, Y., Christophides, G.K., Lelieveld, J., Parham, P.E., 2016. Large-scale modelling of the environmentally-driven population dynamics of temperate aedes albopictus (skuse). PLoS ONE 11 (2), 1–28.

Ewing, D.A., Cobbold, C.A., Purse, B.V., Nunn, M.A., White, S.M., 2016. Modelling the effect of temperature on the seasonal population dynamics of temperate mosquitoes. Journal of Theoretical Biology 400, 65–79. https://doi.org/10.1016/j.jtbi.2016.04.008.

Ewing, D.A., Purse, B.V., Cobbold, C.A., Schäfer, S.M., White, S.M., 2019. Uncovering mechanisms behind mosquito seasonality by integrating mathematical models and daily empirical population data: Culex pipiens in the UK. Parasites and Vectors 12 (1), 1–19.

Ezanno, P., Aubry-Kientz, M., Arnoux, S., Cailly, P., L'Ambert, G., Toty, C., Balenghien, T., Tran, A., 2015. A generic weather-driven model to predict mosquito population dynamics applied to species of anopheles, culex and aedes genera of southern france. Preventive Veterinary Medicine 120 (1), 39–50. https://doi.org/10.1016/j.prevetmed.2014.12.018.

Farnesi, L.C., Martins, A.J., Valle, D., Rezende, G.L., 2009. Embryonic development of aedes aegypti (diptera: Culicidae): Influence of different constant temperatures. Memorias do Instituto Oswaldo Cruz 104 (1), 124–126.

Gelman, A., Rubin, D.B., 1992. A single series from the gibbs sampler provides a false sense of security. Bayesian statistics 4, 625–631.

Hladish, T.J., Pearson, C.A., Patricia Rojas, D., Gomez-Dantes, H., Halloran, M.E., Vazquez-Prokopec, G.M., Longini, I.M., 2018. Forecasting the effectiveness of indoor residual spraying for reducing dengue burden. PLoS Neglected Tropical Diseases 12 (6), 1–16.

Lana, R.M., Carneiro, T.G., Honório, N.A., Codeço, C.T., 2014. Seasonal and nonseasonal dynamics of aedes aegypti in rio de janeiro, brazil: Fitting mathematical models to trap data. Acta Tropica 129 (1), 25–32.

Lana, R.M., Morais, M.M., de Lima, T.F.M., de Senna Carneiro, T.G., Stolerman, L.M., dos Santos, J.P.C., Cortés, J.J.C., Eiras, A.E., Codeço, C.T., 2018. Assessment of a trap based aedes aegypti surveillance program using mathematical modeling. PLoS ONE 13 (1), 1–17.

Leach, C.B., Hoeting, J.A., Pepin, K.M., Eiras, A.E., Hooten, M.B., Webb, C.T., 2020. Linking mosquito surveillance to dengue fever through bayesian mechanistic modeling. PLoS Neglected Tropical Diseases 14 (11), 1–20. https://doi.org/10.1371/journal.pntd.0008868.

Li, R., Xu, L., Bjørnstad, O.N., Liu, K., Song, T., Chen, A., Xu, B., Liu, Q., Stenseth, N.C., 2019. Climate-driven variation in mosquito density predicts the spatiotemporal dynamics of dengue. Proceedings of the National Academy of Sciences of the United States of America 116 (9), 3624–3629.

Marini, G., Guzzetta, G., Baldacchino, F., Arnoldi, D., Montarsi, F., Capelli, G., Rizzoli, A., Merler, S., Rosà, R., 2017. The effect of interspecific competition on the temporal dynamics of aedes albopictus and culex pipiens. Parasites and Vectors 10 (1).

Marini, G., Poletti, P., Giacobini, M., Pugliese, A., Merler, S., Rosà, R., 2016. The role of climatic and density dependent factors in shaping mosquito population dynamics:the case of culex pipiens in northwestern italy. PLoS ONE 11 (4), 1–15. https://doi.org/10.1371/journal.pone.0154018.

Metelmann, S., Caminade, C., Jones, A.E., Medlock, J.M., Baylis, M., Morse, A.P., 2019. The UK's suitability for aedes albopictus in current and future climates. Journal of the Royal Society Interface 16 (152).

Metelmann, S., Liu, X., Lu, L., Caminade, C., Liu, K., Cao, L., Medlock, J.M., Baylis, M., Morse, A.P., Liu, Q., 2021. Assessing the suitability for aedes albopictus and dengue transmission risk in china with a delay differential equation model. PLoS Neglected Tropical Diseases 15 (3), 1–21. https://doi.org/10.1371/journal.pntd.0009153.

Mordecai, E.A., Cohen, J.M., Evans, M.V., Gudapati, P., Johnson, L.R., Lippi, C.A., Miazgowicz, K., Murdock, C.C., Rohr, J.R., Ryan, S.J., Savage, V., Shocket, M.S., Stewart Ibarra, A., Thomas, M.B., Weikel, D.P., 2017. Detecting the impact of temperature on transmission of zika, dengue, and chikungunya using mechanistic models. PLoS Neglected Tropical Diseases 11 (4), 1–18. https://doi.org/10.1371/journal.pntd.0005568.

Nance, J., Fryxell, R.T., Lenhart, S., 2018. Modeling a single season of aedes albopictus populations based on host-seeking data in response to temperature and precipitation in eastern tennessee. Journal of Vector Ecology 43 (1), 138–147.

Oidtman, R.J., Omodei, E., Kraemer, M.U., Castañeda Orjuela, C.A., Cruz-Rivera, E., Misnaza-Castrillón, S., Cifuentes, M.P., Rincon, L.E., Cañon, V., Alarcon, P.d., et al., 2021. Trade-offs between individual and ensemble forecasts of an emerging infectious disease. Nature Communications 12 (1), 1–11.

Perez, J., Bond, C., Buhl, K., Stone, D., 2015. Bacillus thuringiensis (bt) general fact sheet. National Pesticide Information Center, Oregon State University Extension Services.http://npic.orst.edu/factsheets/btgen.html

Petrone, M.E., Earnest, R., Lourenço, J., Kraemer, M.U., Paulino-Ramirez, R., Grubaugh, N.D., Tapia, L., 2021. Asynchronicity of endemic and emerging mosquito-borne disease outbreaks in the dominican republic. Nature Communications 12 (1), 1–12.

Poletti, P., Messeri, G., Ajelli, M., Vallorani, R., Rizzo, C., Merler, S., 2011. Transmission potential of chikungunya virus and control measures: The case of italy. PLoS ONE 6 (5).

Ponlawat, A., Harrington, L.C., 2005. Blood feeding patterns of aedes aegypti and aedes albopictus in thailand. Journal of Medical Entomology 42 (5), 844–849.

Pruszynski, C.A., Hribar, L.J., Mickle, R., Leal, A.L., 2017. A large scale biorational approach using bacillus thuringiensis israeliensis (strain am65-52) for managing aedes aegypti populations to prevent dengue, chikungunya and zika transmission. PloS ONE 12 (2), e0170079.

Robert, M.A., Christofferson, R.C., Silva, N.J., Vasquez, C., Mores, C.N., Wearing, H.J., 2016. Modeling mosquito-borne disease spread in u.s. urbanized areas: The case of dengue in miami. PLoS ONE 11 (8), 1–29. https://doi.org/10.1371/journal.pone.0161365.

Rueda, L.M., Patel, K.J., Axtell, R.C., Stinner, R.E., 1990. Temperature-dependent development and survival rates of culex quinquefasciatus and aedes aegypti (diptera: Culicidae). Journal of medical entomology 27 (5), 892–898.

Simoy, M.I., Simoy, M.V., Canziani, G.A., 2015. The effect of temperature on the population dynamics of aedes aegypti. Ecological Modelling 314, 100–110. https://doi.org/10.1016/j.ecolmodel.2015.07.007.

Stoddard, P.K., 2018. Managing aedes aegypti populations in the first zika transmission zones in the continental united states. Acta Tropica 187, 108–118. https://doi.org/10.1016/j.actatropica.2018.07.031.(June)

Tran, A., L'Ambert, G., Lacour, G., Benoît, R., Demarchi, M., Cros, M., Cailly, P., Aubry-Kientz, M., Balenghien, T., Ezanno, P., 2013. A rainfall- and temperature-driven abundance model for aedes albopictus populations. International Journal of Environmental Research and Public Health 10 (5), 1698–1719.

Tran, A., Mangeas, M., Demarchi, M., Roux, E., Degenne, P., Haramboure, M., Goff, G.L., Damiens, D., Gouagna, L.C., Herbreteau, V., Dehecq, J.S., 2020. Complementarity of empirical and process based approaches to modelling mosquito population dynamics with aedes albopictus as an example-application to the development of an operational mapping tool of vector populations. PLoS ONE 15 (1), 1–21.

Vaidya, A., Bravo-Salgado, A.D., Mikler, A.R., 2014. Modeling climate-dependent population dynamics of mosquitoes to guide public health policies. ACM BCB 2014 - 5th ACM Conference on Bioinformatics, Computational Biology, and Health Informatics, pp. 380–389.

Valdez, L.D., Sibona, G.J., Condat, C.A., 2018. Impact of rainfall on aedes aegypti populations. Ecological Modelling 385, 96–105.(June)

Vehtari, A., Gelman, A., Gabry, J., 2017. Practical bayesian model evaluation using leave-one-out cross-validation and WAIC. Statistics and Computing 27 (5), 1413–1432.

Vehtari, A., Simpson, D., Gelman, A., Yao, Y., Gabry, J.. Pareto smoothed importance sampling. arXiv:1507.02646.

White, M.T., Griffin, J.T., Churcher, T.S., Ferguson, N.M., Basáñez, M.G., Ghani, A.C., 2011. Modelling the impact of vector control interventions on anopheles gambiae population dynamics. Parasites and Vectors 4 (1), 1–14.

Wilke, A.B., Carvajal, A., Medina, J., Anderson, M., Nieves, V.J., Ramirez, M., Vasquez, C., Petrie, W., Cardenas, G., Beier, J.C., 2019. Assessment of the effectiveness of BG-sentinel traps baited with CO2 and BG-lure for the surveillance of vector mosquitoes in miami-dade county, florida. PLoS ONE 14 (2), e0212688.

Wilke, A.B., Chase, C., Vasquez, C., Carvajal, A., Medina, J., Petrie, W.D., Beier, J.C., 2019. Urbanization creates diverse aquatic habitats for immature mosquitoes in urban areas. Scientific Reports 9 (1), 1–11.

Wilke, A.B., Vasquez, C., Carvajal, A., Moreno, M., Fuller, D.O., Cardenas, G., Petrie, W. D., Beier, J.C., 2021. Urbanization favors the proliferation of aedes aegypti and culex quinquefasciatus in urban areas of miami-dade county, florida. Scientific reports 11 (1), 1–12.

Wilke, A.B., Vasquez, C., Carvajal, A., Ramirez, M., Cardenas, G., Petrie, W.D., Beier, J. C., 2021. Effectiveness of adulticide and larvicide in controlling high densities of aedes aegypti in urban environments. PLoS ONE 16 (11), 1–15.

Wilke, A.B., Vasquez, C., Medina, J., Carvajal, A., Petrie, W., Beier, J.C., 2019. Community composition and year-round abundance of vector species of mosquitoes make miami-dade county, florida a receptive gateway for arbovirus entry to the united states. Scientific reports 9 (1), 1–10.

Wilke, A.B.B., Vasquez, C., Carvajal, A., Medina, J., Chase, C., Cardenas, G., Mutebi, J.-P., Petrie, W.D., Beier, J.C., 2020. Proliferation of aedes aegypti in urban environments mediated by the availability of key aquatic habitats. Scientific Reports 10 (1), 1–10.

Williams, K.K., Ramirez, S., Lesser, C.R., 2022. Field evaluation of wals truck-mounted a1 super duty mist sprayer® with vectobac® wdg against aedes aegypti (diptera: Culicidae) populations in manatee county, florida. SN Applied Sciences 4 (2), 1–15.

Yang, H.M., Macoris, M.L., Galvani, K.C., Andrighetti, M.T., Wanderley, D.M., 2009. Assessing the effects of temperature on the population of aedes aegypti, the vector of dengue. Epidemiology and Infection 137 (8), 1188–1202.

Yé, Y., Sauerborn, R., Séraphin, S., Hoshen, M., 2007. Using modelling to assess the risk of malarial infection during the dry season, on a local scale in an endemic area of rural burkina faso. Annals of Tropical Medicine and Parasitology 101 (5), 375–389.

Yi, B., Chen, Y., Ma, X., Rui, J., Cui, J.A., Wang, H., Li, J., Chan, S.F., Wang, R., Ding, K., Xie, L., Zhang, D., Jiao, S., Lao, X., Chiang, Y.C., Su, Y., Zhao, B., Xu, G., Chen, T., 2019. Incidence dynamics and investigation of key interventions in a dengue outbreak in ningbo city, china. PLoS Neglected Tropical Diseases 13 (8), 1–23.